Research

New Phytologist

E3 ligase ATL5 positively regulates seed longevity by mediating the degradation of ABT1 in *Arabidopsis*

Wenping He[1], Run Wang[1], Qi Zhang[1], Mingxia Fan[1], Yuanyuan Lyu[1], Shuai Chen[1], Defu Chen[2] and Xiwen Chen[1]

[1]Department of Biochemistry and Molecular Biology, College of Life Sciences, Nankai University, Tianjin, 300071, China; [2]Department of Genetics and Cell Biology, College of Life Sciences, Nankai University, Tianjin, 300071, China

Authors for correspondence:
Defu Chen
Email: chendefu@nankai.edu.cn

Xiwen Chen
Email: xiwenchen@nankai.edu.cn

Received: *16 November 2022*
Accepted: *10 May 2023*

New Phytologist (2023) **239:** 1754–1770
doi: 10.1111/nph.19080

Key words: activator of basal transcription 1, *Arabidopsis*, ATL5, E3 ligase, seed longevity, ubiquitination.

Summary

- Ubiquitination is a fundamental mechanism regulating the stability of target proteins in eukaryotes; however, the regulatory mechanism in seed longevity remains unknown. Here, we report that an uncharacterized E3 ligase, ARABIDOPSIS TÓXICOS EN LEVADURA 5 (ATL5), positively regulates seed longevity by mediating the degradation of ACTIVATOR OF BASAL TRANSCRIPTION 1 (ABT1) in *Arabidopsis*.
- Seeds in which ATL5 was disrupted showed faster accelerated aging than the wild-type, while expressing *ATL5* in *atl5-2* basically restored the defective phenotype. *ATL5* was highly expressed in the embryos of seeds, and its expression could be induced by accelerated aging.
- A yeast two-hybrid screen identified ABT1 as an ATL5 interacting protein, which was further confirmed by bimolecular fluorescence complementary assay and co-immunoprecipitation analysis. *In vitro* and *in vivo* assays showed that ATL5 functions as an E3 ligase and mediates the polyubiquitination and degradation of ABT1. Disruption of ATL5 diminished the degradation of translated ABT1, and the degradation could be induced by seed ageing and occurred in a proteasome-dependent manner. Furthermore, disruption of ABT1 enhanced seed longevity.
- Taken together, our study reveals that ATL5 promotes the polyubiquitination and degradation of the ABT1 protein posttranslationally and positively regulates seed longevity in *Arabidopsis*.

Introduction

As a carrier of plant genetics and sexual reproduction, seeds are an important strategy for plant adaptation to the natural environment and the foundation of great agriculture. However, seed aging or seed deterioration is an inevitable and irreversible process during storage. Seed longevity, the period over which orthodox seeds maintain vigor and germination ability in a dry state (de Souza *et al.*, 2016), is crucial for both ecological and agronomic value. Identifying genes, especially regulatory genes, involved in seed longevity and understanding the mechanism of action are, therefore, vital for the preservation of germplasm resources and food safety.

Seed longevity is acquired during seed development, reaches the highest peak when seeds mature, and gradually declines during seed storage. A series of cellular and physiological processes occur in the embryo during seed maturation (Leprince *et al.*, 2017). The water content in seeds gradually decreases, and the cytoplasm becomes glassy (Leprince *et al.*, 2017). Chlorophyll and carotenoids in seeds degrade (Clerkx *et al.*, 2003). The composition and content of soluble sugars also change (Verdier *et al.*, 2013; Wang *et al.*, 2018). The transcription of HEAT SHOCK PROTEIN (HSP) and SMALL HSP (sHSP) genes is induced, and LATE EMBRYOGENESIS ABUNDANT PROTEIN (LEA) accumulates in late embryonic development (Leprince *et al.*, 2017). Despite the extremely low metabolic activity in dry seeds, amadori and Maillard (Murthy & Sun, 2000), lipid peroxidation (Wiebach *et al.*, 2020), protein carbonylation (Rajjou *et al.*, 2011), and other reactions still inevitably occur in cellular components (proteins, lipids, nucleic acids, sugars, etc.). Antioxidant systems, including passive nonenzymatic scavenging systems (Sano *et al.*, 2016) and active enzymatic detoxification systems (Jeevan *et al.*, 2015), prevent excessive oxidation of biological macromolecules and play a significant role in seed longevity.

The transcriptional regulation mechanisms involved in seed longevity during seed development have mostly been reported. The transcriptional activators LAFL (LEAFY COTYLEDON1, LEC1; ABA INSENSITIVE3, ABI3; FUSCA3, FUS3; LEC2) and plant hormones, such as abscisic acid (ABA) and its signaling pathways, form a complex network and regulate multiple downstream processes related to seed longevity (Sano *et al.*, 2016). For example, ABI3 activates the gene expression of the key enzymes NONYELLOW COLORING1 (NYC1) and NONYELLOW

COLORING1-like (NOL) in the chlorophyll decomposition pathway (Nakajima *et al.*, 2012). raffinose family oligosaccharides (RFO) synthesis is also regulated at the transcriptional level (Downie *et al.*, 2003). The RFO level in *Arabidopsis* (*Arabidopsis thaliana*) *abi3* and *aba1 abi3* mutant seeds is lower than that of the wild-type, and exogenous ABA can stimulate RFO accumulation (Dekkers *et al.*, 2016). The expression of HSP (heat shock protein) is regulated by the seed-specific transcription factor HEAT SHOCK FACTOR A9 (HSFA9), which is regulated by ABI3 (Kotak *et al.*, 2007), ABI5 and DELAY OF GERMINATION 1 (DOG1; Dekkers *et al.*, 2016). The transcription of LEA genes is also regulated by a network of transcription factors, including ABI3, ABI4, ABI5, and DOG1 (Reeves *et al.*, 2011; Dekkers *et al.*, 2016). Recently, a multiomic study uncovered a bZIP23-PER1A-mediated detoxification pathway to enhance seed vigor in rice (Wang *et al.*, 2022). However, it is still unclear whether other regulatory mechanisms are involved in seed longevity-related processes.

Ubiquitination is a common posttranslational protein modification in eukaryotes that is an efficient and rapid mechanism for fine-regulating the stability of target proteins and plays a critical role in various biological processes (Ciechanover, 2015). Ubiquitination involves an enzymatic cascade composed of E1 (Ub (UBIQUITIN)-activating enzyme), E2 (Ub CONJUGATING ENZYME), and E3 (Ub LIGASE). The *Arabidopsis* genome contains 2 E1, 47 E2s and > 1400 E3s (Liu *et al.*, 2017). The large number of E3 ligase genes indicates that E3 ligases are key factors in the ubiquitination process and determine substrate specificity (Hershko & Ciechanover, 1998). ARABIDOPSIS TÓXICOS EN LEVADURA (ATLs) are a plant-specific REALLY INTERESTING NEW GENE (RING)-type E3 ligase family. The *Arabidopsis* genome contains 91 ATL members (Smalle & Vierstra, 2004). The protein contains a RING-H2-type zinc finger domain and 1 or 2 hydrophobic transmembrane domains in the N-terminus (Sato *et al.*, 2011). Several ATL isoforms have been reported to function in biotic and abiotic stress responses. For example, AtATL2 expression can be rapidly induced by pathogens and plays a role in salicylic acid- and jasmonic acid-mediated defenses (Serrano & Guzman, 2004). AtATL9 is involved in chitin- and NADPH oxidase-mediated defense responses (Deng *et al.*, 2017). AtATL78 is a negative regulator of the cold stress response and a positive regulator of the drought stress response, mediating ABA-dependent stomatal closure (Suh *et al.*, 2016). Several ATL isoforms are also involved in plant development and the absorption and transport of mineral nutrients. AtATL49 regulates embryonic development (Pagnussat *et al.*, 2005), and AtATL62 is involved in the photoperiod response (Morris *et al.*, 2010). ATL31 and ATL6 also regulate the carbon/nitrogen balance by degrading 14-3-3χ protein (Sato *et al.*, 2011). AtATL14 regulates iron homeostasis through ubiquitination and degradation of IRT1 (IRON-REGULATED TRANSPORTER1; Shin *et al.*, 2013). AtATL80 expression could be induced by low Pi (0–0.02 mM), and its overexpression lines increased phosphorus accumulation and decreased phosphorus utilization efficiency (Suh & Kim, 2015). However, most ATL family members have not been studied, and their functions remain unknown.

RNA polymerase II (Pol II)-mediated transcription is an orchestrated process that requires the concerted functions of general transcription factors (GTFs), sequence-specific activators or repressors, and accessory proteins. The transcription factor II D (TF IID) complex is composed of TATA box-binding protein (TBP) and TBP-associated factors (TAFs), and TBP is the first GTF that binds to the promoter during transcription initiation. Several TBP-binding proteins have been identified to play important roles in both basal and specific transcription of gene expression (Heiss *et al.*, 2019). Yeast ACTIVATOR OF BASAL TRANSCRIPTION 1 (ABT1) was first identified as a novel TBP binding protein and promotes Pol II-mediated basal transcription *in vitro* and in HeLa cells (Oda *et al.*, 2000). Sequence alignment revealed that ABT1s contain a unique acidic region, which has been described as a transcriptional activation domain in many transcription factors, such as VP16, GAL4, GCN4, and P53 (Oda *et al.*, 2004; Maeda *et al.*, 2017). No plant ABT1 has been described except *Arabidopsis* ATB1 (designated TBP binding protein), which was found to be upregulated in a microarray analysis (Li *et al.*, 2007), and its protein phosphorylation hotspots were predicted (Christian *et al.*, 2012). In this study, we report that ATL5 functions as an E3 ligase, mediates the polyubiquitination and degradation of ABT1, and positively affects seed longevity in *Arabidopsis*. Our results provide insights into an uncharacterized E3 ligase regulating a basal transcription activator governing seed longevity that could serve as new target for improving orthodox seed longevity in crops.

Materials and Methods

Plant growth conditions

Arabidopsis thaliana T-DNA insertion mutants *atl5-2* (SALK-114494), *abt1-1* (SALK_044704C), *lig4-1* (DNA ligase IV, SALK_026361C), *lig6-1* (DNA ligase VI, SALK_060665), *bg14-1* (*β-1,3-GLUCANASE 14*, SALK_068499), *aba 1–1* (zeaxanthin epoxidase, SALK_059469), and *higd2-2* (hypoxia-inducible gene domain family member 1, SALK_018276) (all in Col-0 background, simply referred to by their gene abbreviations henceforth) were obtained from the *Arabidopsis* Biological Resource Center (https://abrc.osu.edu) or Arashare (https://www.arashare.cn). Transgenic promoter-GUS line *ProATL5:GUS*, functional reversion (*ATL5*-RE) and overexpression (*ATL5*-OE) transgenic lines of *ProATL5:ATL5-Ac* (*Aequorea coerulescens*) *GFP*, and *35S:ABT1-MYC* (*ABT1*-OE) were generated by using the methods described below.

Seeds were germinated on plates containing ½ Murashige & Skoog medium (½MS). After 3 d of moist chilling at 4°C, the plates were placed in a growth chamber with 16 h of 275 μmol m^{-2} s^{-1} light and 8 h of dark at 22°C for 2 wk. Seedlings were then transplanted into nutrient soil and cultured in an incubator under the same conditions for *c.* 3 months to complete the life cycle. *Nicotiana benthamiana* plants were also grown in an incubator under the same conditions.

Isolation of T-DNA insertion mutant lines

Genomic DNA was isolated from leaf tissues of different genotypes using a modified cetyltrimethylammonium bromide (CTAB) method (Murray & Thompson, 1980). Homozygous mutants were screened by PCR using primers recommended by the SALK primer design tool (http://signal.salk.edu/tdnaprimers.2.html; Supporting Information Table S1). Total RNA was isolated from the leaves of homozygous plants using an RNAiso Plus kit (TaKaRa Biotechnology (Dalian) Co. Ltd, Dalian, China). cDNAs were synthesized using Reverse Transcriptase M-MLV (TaKaRa) and SMART 3′-end primers. The expression levels of *ATL5* (783 bp) and *ABT1* (782 bp) were assessed using the primer pairs atl5-Nde-F/atl5-Pst-R and 56 510-F/56510-Bgl-R, respectively, while a 515-bp fragment of ACT2 (515 bp) was amplified as the quantitative control using AtActin-qF3/AtActin-R4 (Table S1).

Controlled deterioration treatment and germination assay

Seed longevity was evaluated by controlled deterioration treatment (CDT; Renard *et al.*, 2020). Seeds that were collected and stored dry in paper bags at room temperature for at least 1 month were used for the experiment. Seeds put in microcentrifuge tubes with lids removed were placed on a copper wire-mesh tray above 130 ml of saturated NaCl solution with 0.01% NaClO inside a plastic aging boxes (12.2 cm × 12.2 cm × 4.8 cm) (Zhejiang Top Cloud-Agri Technology Co. Ltd, Hangzhou, China) and the lid sealed. After 2 d of water equilibrium at room temperature (25 ± 1°C), CDT was performed in a seed aging tank (Zhejiang Top Cloud-Agri Technology) at 42°C with 70% RH for 4 d (4CDT). Seeds were then dried at 25 ± 1°C for 2 d before the germination assay and tetrazolium assay were performed. Aged seeds were sown on ½MS solid medium and moist chilled at 4°C for 3 d. Germination was performed as described above and recorded daily until the 7th day. Seeds were considered to have completed germination when they showed a > 2 mm radicle. The mean germination time (MGT) was calculated based on the equation (Matthews & Khajeh-Hosseini, 2007): $MGT = \Sigma(f \times i)/\Sigma f$, where f is the number of seeds completing germination on day i.

Tetrazolium assay

To detect viable seeds, a tetrazolium (TTZ, 2,3,5-triphenyl tetrazolium chloride) assay was performed as described by Rao *et al.* (2018) with minor modifications. In short, seeds were slightly scratched with an emery cloth, soaked in 1% TTZ solution at 30°C for 48 h and then washed twice with distilled water. Pictures were taken using a Leica S9i stereomicroscope (Leica Microsystems Co. Ltd, Wetzlar, Germany).

Vector construction and generation of transgenic plants

The 2261 bp promoter of *ATL5* (ATL5 P-1 and ATL5 P-2) was amplified using the primers atl5-F1/atl5-R1 and atl5-F2/atl5-R2, respectively (Table S1). The ATL5 P-2 fragment was first inserted into pCAMBIA3301 using the *Eco*RI/*Nco*I site, and then the ATL5P-1 fragment was inserted using *Eco*RI sites to produce the *ProATL5:GUS* construct. The full-length ATL5 open reading frame was amplified from leaf DNA using the primers atl5-PB-F/atl5-Pst-R, inserted into pT-GFP-PB (kept in our laboratory) using the *Pst*I site to generate pT-atl5-GFP, and then inserted into the *ProATL5:GUS* vector using the *Bgl*II site to produce the *ProATL5:ATL5-GFP* constructs. For *35S:ABT1-MYC*, the coding sequence (CDS) of ABT1 was amplified using primers 56510-Bgl-F/56510-Bgl-R (Table S1) and then inserted into *p3301-MYC* (assembled primers MYC-F/MYC-R with pCAMBIA3301) using the *Bgl*II site.

These constructs were subsequently transformed into *Agrobacterium tumefaciens* LBA4404 by electroporation. Transgenic plants were generated by the standard floral dip method (Clough & Bent, 1998) to transform the wild-type and mutant plants. The transformants were selected by spraying basta (glufosinate ammonium) onto T_1 seedlings and purified by multiple generations of self-crossing.

Quantitative real-time PCR analysis

Total RNA was isolated using an Eastep™ Super Total RNA Extraction kit (Shanghai Promega Biological Products Co. Ltd, Shanghai, China). After treatment with DNase I (TaKaRa), reverse transcription was performed using M-MLV (TaKaRa) at 42°C for 60 min and then inactivation at 70°C for 15 min. qRT–PCR was performed using the products as templates and ATL5-qRT-F/ATL5-qRT-R as primers on a CFX Connect™ Real-time PCR System (Bio-Rad). Each reaction contained 10 µl 2 × SYBR Premix *Ex Taq*™ II buffer, 1 µg cDNA and 10 µmol of each pair of primers for specific targets (Table S1) in a final volume of 20 µl. A 113 bp sequence of ACT2 was used as an internal control to normalize the data using AtActin qR3/AtActin-qF3 (Table S1) as primers.

GUS staining

Seedlings, flowers, siliques, and seeds at different developmental stages were collected. After fixing with 90% acetone for 20 min at room temperature, tissue samples were then incubated overnight in a GUS staining solution (100 mM phosphate buffer (pH 7.0), 1 mM X-gluc, 10 mM EDTA, 0.1% (v/v) Triton X-100) at 37°C. Images were directly photographed or after washing with 75% (v/v) ethanol to remove chlorophyll using a Leica S9i stereomicroscope (Leica Microsystems Co. Ltd).

Protoplast isolation and subcellular location

The CDS of ATL5 was amplified using atl5-PB-F/atl5-Bam-R (Table S1) and introduced into pHBT-GFP-NOS to generate pHBT-ATL5-GFP. *Arabidopsis* leaf mesophyll protoplasts were isolated from 3- to 4-wk-old seedlings as described previously (Yoo *et al.*, 2007). Plasmids (3–10 µg each) of pHBT-ATL5 and NLS (nuclear localization signal)-mCherry (as nuclear markers)

were cotransformed into 200 µl protoplasts by 40% PEG-calcium transfection solution (Yoo *et al.*, 2007). After culturing at 22°C for 14–16 h, the fluorescence signal was detected by a laser confocal microscope LSM710 (Carl Zeiss Optical (Guangzhou) Co. Ltd, Guangzhou, China).

Yeast two-hybrid screening and assays

The open reading frame without the transmembrane domain of ATL5 was amplified using the primers atl5-Nde-F2/atl5-Pst-R2 (Table S1) from genomic DNA and then subcloned into pGBKT7 to generate BD-ATL5. BD-ATL5 was used as a 'bait' to screen against a normalized *Arabidopsis* Y2H cDNA library (Clontech Laboratories, Inc., Waltham, MA, USA) according to the manufacturer's guidelines. After 20 h of conjugation, selections were sequentially performed on SD-Trp-Leu-His medium plus 2 mM 3-AT (Beijing Coolaber Technology Co. Ltd, Beijing, China) and SD-Trp-Leu-His-Ade medium with 2 mM 3-AT. Positive clones were then assessed for their β-galactosidase activity on SD-Trp-Leu-His-Ade plates plus 4 mg ml^{-1} X-α-Gal (Beijing Coolaber Technology Co. Ltd) and 2 mM 3-AT at 30°C for 4 d. Blue clones were used for colony PCR using the primer pair T7/3AD (Table S1), and the products were sequenced and aligned in NCBI (https://blast.ncbi.nlm.nih.gov/Blast.cgi). After obtaining the candidate interacting proteins, PLANT-MPLOC (http://www.csbio.sjtu.edu.cn/bioinf/plant/) and Arabidopsis eFP Browser were used to predict their subcellular localization and tissue-specific expression pattern (Table S2). Eight putative proteins were selected for specific interaction confirmation. The coding regions of ATL5 (without the transmembrane domain), ATL5-D1 (51–154 aa), and ATL5-D2 (153–257 aa) were amplified using atl5-Nde-F2/atl5-Bam-R2, atl5-Nde-F2/atl5-D1-R, and atl5-D2-F/atl5-Bam-R2, respectively (Table S1), and the coding sequences of full-length ABT1, ABT1-D1 (1–49 aa), ABT1-D2 (50–146 aa), and ABT1-D3 (147–257 aa) were amplified using 56 510-F/56510-R, 56510-F/56510-D1-R, 56510-D2-F/56510-D2-R, and 56 510-D3-F/56510-R, respectively (Table S1). ATL5 or truncated domains were fused to pGADT7, and full-length or truncated forms of ABT1 were inserted into pGBKT7. To test the interaction of TBP1 or TBP2 with ABT1, the full-length coding sequences of TBP1 or TBP2 were amplified using TBP1-Nde-F/TBP1-Bam-R or TBP2-Nde-F/TBP2-Bam-R, respectively, and then fused to pGADT7. The plasmids were cotransformed into the Y2H gold yeast strains and cultured on SD-Trp-Leu-His-Ade plates. pGADT7 (AD) and pGBKT7 (BD) vectors were used as negative controls.

Bimolecular fluorescence complementation assays

The full-length CDSs of *ATL5* and *ABT1* were amplified using the primers atl5-Spe-F/atl5-Kpn-R and 56 510-Spe-F/56510-Kpn-R, respectively. Then, the PCR products were fused to the C-terminal- or N-terminal-yellow fluorescent protein (YFP) fragment (ATL5-cYFP) driven by the cauliflower mosaic virus (CaMV) 35S promoter of pSPYCE-35S and pSPYNE-35S to generate YC-ATL5 and YN-ABT1, respectively. YC-ATL5, YN-ABT1, and NLS-mCherry (nuclear markers) were co-transformed into 4- to 7-wk-old *N. benthamiana* leaves using the *A. tumefaciens* method (Waadt & Kudla, 2008). After 3 d, the YFP signal was observed under a confocal microscope (Zeiss LSM710).

Expression and purification of GST-tagged ATL5 protein and *in vitro* ubiquitination analysis

The *ATL5* open reading frame without the transmembrane domain was amplified using primers atl5-BamHI-D50F/atl5-SalI-R (Table S1) and subcloned into pGEX6P-1 using *Bam*HI/*Sal*I sites. The resulting *ATL5-GST* vector was transformed into *Escherichia coli* BL21(DE3) and induced by l mM IPTG overnight at 16°C. The recombinant proteins were affinity purified from bacterial lysates using GSTSep Glutathione Agarose Resin (Yeasen Biotechnology (Shanghai) Co. Ltd, Shanghai, China) according to the manufacturer's instructions.

In vitro ubiquitination analysis was completed as described by Sato *et al.* (2009) with minor modifications. Briefly, *c.* 500 ng purified ATL5-GST protein was mixed with 40 ng yeast E1 (uba1), 250 ng yeast E2 (rad6), and 9 ng yeast ubiquitin in a 40 µl reaction and incubated at 30°C for 3 h. After separation by 12.5% SDS–PAGE, proteins were transferred to polyvinylidene fluoride membranes and immunoblotted using an anti-ubiquitin antibody (Proteintech Group Inc., Chicago, IL, USA). The protein blots were developed with an ECL Detection Kit (Invitrogen), and images were scanned using a Tanon 5200 Chemiluminescence Imaging System (Millipore). The intensity of the images was quantified by IMAGEJ (National Institute of Health).

Co-immunoprecipitation (Co-IP) assay, semi-*in vitro* ubiquitination and protein degradation analysis in *Nicotiana benthamiana*

The full-length ORFs of *ATL5* and *ABT1* were amplified with the primers myc-atl5-B-R/atl5-PB-F and 56 510-Spe-F/56510-Kpn-R (Table S1) and then inserted into pCAMBIA3301 and pCanG-3FLAG to generate *ATL5-MYC* and *ABT1-FLAG*, respectively. AcGFP was also amplified using AcGFP-Kpn-R/AcGFP-Xba-F (Table S1) and inserted into pCanG-3FLAG to generate *GFP-FLAG*. *Agrobacterial strains* carrying constructs *ABT1-FLAG*, *ATL5-MYC*, or *GFP-FLAG* were infiltrated into tobacco leaves according to the method described by Liu *et al.* (2010). After 3 d, proteins were extracted from leaves using a plant protein extraction kit (Beijing ComWin Biotech Co. Ltd, Beijing, China). Co-IP assays were performed using whole protein extracts as described previously (Gao *et al.*, 2021). The ATL5-MYC protein was immunoprecipitated with 5 µg anti-MYC (Proteintech Group Inc.), 50 µM MG132 and 50 µl Beyo-Mag™ Protein A + G Beads (Beyotime Biotech Inc., Shanghai, China) at 4°C overnight. The co-immunoprecipitated ABT1-FLAG was detected using an anti-FLAG antibody (Proteintech Group Inc.). The protein blots were developed, scanned, and quantified as described above.

For semi *in vitro* ubiquitination analysis, protein was extracted from the infiltrated leaves. After adding 20 µl BeyoMag™ protein A + G beads (Beyotime), the sample mixture was incubated at 4°C for 2 h, centrifuged at 14 000 ***g*** for 1 min to obtain the ABT1-FLAG/ATL5-MYC complex and dissolved in 900 µl of 50 mM Tris–HCl (pH 7.5). Semi *in vitro* ubiquitination analysis was performed by adding 4 µg yeast ubiquitin, 50 ng yeast E1 (uba1) or/and 100 ng yeast E2 (rad6) and 30 µl protein extracts and incubating at 30°C for 90 min. Immunoblotting assays were performed and quantified as described above.

In planta and *in vivo* protein degradation assay

For *35S:ATL5C132A-MYC* vector construction, ATL5C132A was first amplified using pT-atl5-ORF as a template and atl5-PB-F/atl5-C132A-R and atl5-C132A-F/atl5-Pst-R as primers (Table S1). Then, the products were mixed at a ratio of 1 : 1, used as a template to amplify ATL5C132A using atl5-PB-F/atl5-pst-R as primers (Table S1), and inserted into P3301-atl5-MYC by *Eco*RI/*Hin*dIII to generate ATL5C132A-MYC. Different combinations of *Agrobacterium strains* carrying constructs *ABT1-FLAG* and *ATL5-MYC* or *ATL5C132A-MYC* were co-infiltrated with *N. benthamiana* leaves according to the method described in Liu *et al.* (2010), and *GFP-FLAG* was used as an internal expression control. Samples were collected after 3 d. Fifty micromolar cycloheximide (CHX) and/or 50 µM MG132 were injected into leaves 12 h before sampling. Proteins were extracted and subjected to immunoblotting with anti-MYC (Proteintech Group Inc.), anti-FLAG (Proteintech Group Inc.), and anti-GFP (Proteintech Group Inc.) antibodies. The *in planta* protein degradation assay was performed according to the method described by Li *et al.* (2020).

For the degradation of ABT1 in *Arabidopsis* seeds, seeds of *ABT1-MYC::Col-0* and *ABT1-MYC::atl5* transgenic plants were collected. After aging treatment and moist chilling, seeds (0.2 g each) were placed in 1/2 liquid MS medium without or with 50 µM CHX or/and 50 µM MG132, and cultured at 22°C for 2 h. Total protein was extracted using a Protein Extraction Kit (Beijing ComWin Biotech Co. Ltd). ABT1-MYC protein levels were analyzed by Western blotting using an anti-MYC antibody (Proteintech Group Inc.). The protein blots were developed, scanned, and quantified as described above. Plant-actin (Boaoyijie (Beijing) Technology Co. Ltd, Beijing, China) was used as an internal control.

Gene accessions

Genes referenced in this article can be found in the *Arabidopsis* Information Resource (TAIR) under the following accession nos.: ATL5 (AT3G62690), ABT1 (AT3G56510), CLC2 (AT2G40060), U3 containing 90S preribosomal complex subunit (AT2G43110), PUX10 (AT4G10790), GTE6 (AT3G52280), PHOS32 (AT5G54430), Y14 (AT1G51510), DUF1639 (AT4G20300), TBP1 (AT3G13445), TBP2 (AT1G55520), LIG 4 (AT1G49250), LIG 6 (AT1G66730), BGL14 (AT2G27500), ABA1 (AT5G67030), HIGD2 (AT5G27760), and ACT2 (At3G18780).

Results

Loss of function of ATL5 showed faster accelerated seed aging in *Arabidopsis*

Our previous global transcriptomics analysis revealed that *OsATL26* (*Os02g0572200*) was significantly upregulated in accelerated aged rice seed embryos of RNAi rice plants constitutively silenced for homogentisate phytyltransferase, homogentisate geranylgeranyl transferase, or tocopherol/tocotrienol cyclase, which showed decreased seed longevity compared with the wild-type (Chen *et al.*, 2016). The *Arabidopsis* homologous gene of *OsATL26* is *AT3G62690*, which encodes the ATL5 protein, a member of the RING finger E3 ligase family.

To investigate the function of ATL5 in seed longevity, an *atl5-2* mutant, which contains a T-DNA insertion in the exon of ATL5, was obtained (Fig. 1a). The homozygous mutants were screened by PCR and RT–PCR analysis (Fig. 1b,c). The seeds of the wild-type (WT) and *atl5-2* mutant were treated with 4CDT, and unaged seeds were used as controls to compare their germination percentage and MGT. The unaged WT and *atl5-2* seeds began to complete germination at 1 days after moist chilling (DAM) and reached 96.0% vs 97.0% (WT at 4 vs 7 DAM) and 92.3% vs 94.0% (*atl5-2* at 4 vs 7 DAM), respectively (Fig. 1d,e). No significant difference was shown in the germination percentage before aging treatment. After 4CDT, the germination percentage of WT was 29.7% at 7 DAM, while that of *atl5-2* was only 2.2% at 7 DAM (Fig. 1d,e). Meanwhile, *atl5-2* was slower to germinate as indicated by significantly higher MGT than WT (5.3 vs 3.6) after 4CDT, while no difference was shown between WT and *atl5-2* seeds (2.1–2.2) before ageing treatment (Fig. 1f). These results indicated that loss of function of ATL5 showed faster seed accelerated aging in *Arabidopsis*.

ATL5 strongly and positively regulates seed longevity in *Arabidopsis*

To further confirm the function of ATL5 in seed longevity, we transformed the *ATL5-GFP* fusion gene driven by its own promoter or cauliflower mosaic virus 35S (Fig. 2a) into the *atl5-2* mutant or WT to generate reversion (*ATL5*-RE) and overexpression (*ATL5*-OE) lines, respectively. The expression levels of *ATL5* in transgenic lines were detected by quantitative real-time polymerase chain reaction (qRT-PCR). For simplicity, we chose the *ATL5*-RE lines (RE-3 and RE-20) with the same expression level as WT (Fig. S1a) and the *ATL5*-OE lines (OE-22 and OE-24) with the highest expression level (Fig. S1b) for subsequent experiments after purification by several cycles of self-pollination.

The unaged WT, *atl5-2*, *ATL5*-RE, and *ATL5*-OE seeds showed no significant difference in the germination percentage at each time point, which began to complete germination at 1 DAM, and the germination percentage reached 84.4–92.2% at 3 DAM (Figs 2b, S2a). After 4CDT, the germination percentage of WT was 17.9% at 7 DAM, while that of *atl5-2* was 0 at 7 DAM. Expression of ATL5 in the *atl5-2* mutant (*ATL5*-RE) restored the faster accelerated ageing phenotype of the mutant, while overexpression of

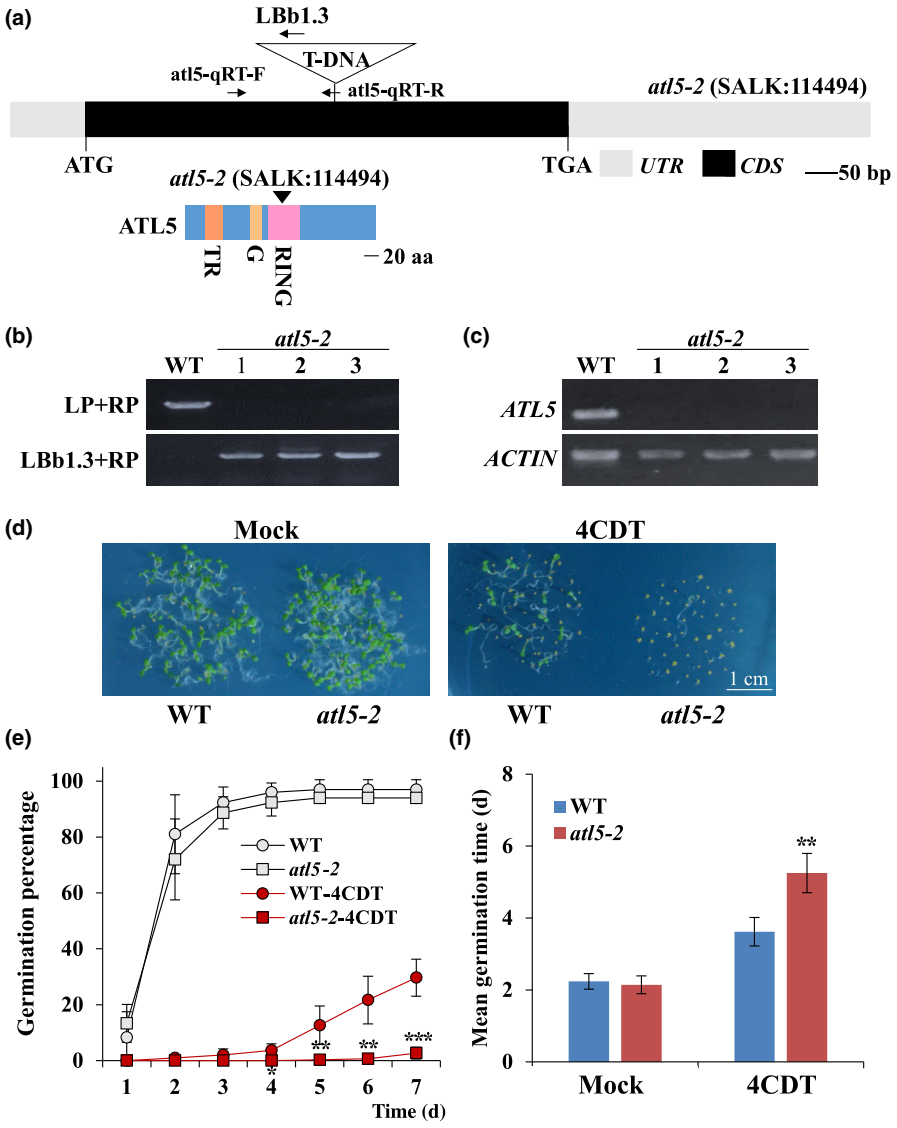

Fig. 1 Loss of function of ATL5 leads to faster accelerated aging in *Arabidopsis* (*Arabidopsis thaliana*). (a) T-DNA insertion diagram in the gene or protein of the *atl5-2* mutant. The black box represents the coding sequence (CDS), the gray box represents UTRs, and the inverted triangle represents insertion sites. The blue box represents the protein, the colored boxes represent the conserved motifs. TR, transmembrane region; G, highly conserved motif containing Gly-Leu-Asp residues; RING, RING-H2 type zinc finger domain. (b) PCR analysis of the wild-type (WT) and *atl5-2* mutant. LP, left primer; RP, right primer; LBb1.3, T-DNA left border primer. (c) RT–PCR analysis of the WT and *atl5-2* mutant, using atl5-qRT-F and atl5-qRT-R primers. Germination status (d), percentage (e) and mean germination time (MGT) (f) of WT and *atl5-2* mutant seeds without (mock) or with 4 d of controlled deterioration treatment (4CDT). Pictures were taken at 7 days after moist chilling (DAM). Bar, 1 cm. Data are shown as the mean ± SD ($n = 3$). Asterisks above or below the bars indicate significant differences with the respective control (*t*-test): *, $P < 0.05$; **, $P < 0.01$; ***, $P < 0.001$.

ATL5 in WT increased the seed germination percentage to 39.8% at 7 DAM (Figs 2b, S2a). Meanwhile, expression of ATL5 in the *atl5-2* mutant restored the higher MGT to that of WT after 4CDT (Fig. 2c). Furthermore, viable seeds revealed by TTZ staining corresponded well with the respective seed aging phenotype in these genotypes (Fig. 2d). Moreover, WT, *atl5-2*, *ATL5*-RE, and *ATL5*-OE showed no phenotypic difference during the growth and development stages (Fig. S3). These results clearly demonstrate that ATL5 positively regulates seed longevity in *Arabidopsis*.

To further investigate the effect of ATL5 on seed longevity, we compared the seed aging phenotype with several T-DNA mutants of genes that have been reported (*aba1*, *lig4*, *lig6*) (Waterworth *et al.*, 2010; Dekkers *et al.*, 2016) or are currently studied in our lab (*bg14*, *higd2*) to function in seed longevity. Similarly, the unaged WT and mutant seeds showed no significant difference in the germination percentage at any time point (Figs 2e, S2b). After 4CDT, the germination percentage of *atl5-2* was 8.6% at 7 DAM, which was significantly lower than those of the other five mutants (25.7–37.6%) at 7 DAM (Figs 2c, S2b). Meanwhile, *atl5-2* had almost the highest MGT among these mutants, except a slightly lower MGT than *lig4* and *lig6* (Fig. S2c). Correspondingly, viable seeds revealed by TTZ staining were also consistent with the respective seed aging phenotype in these mutants (Fig. S2d). Taken together, these results indicated that ATL5 strongly and positively regulates seed longevity in *Arabidopsis*.

ATL5 is highly expressed in seeds and can be induced by accelerated aging, and the protein is located in the nucleus

To better understand the function of ATL5 in seed longevity, we detected the tissue-specific expression of *ATL5*. A 2261 bp promoter of ATL5 was cloned, the *ProATL5:GUS* vector was constructed (Fig. 3a), and 19 independent transgenic lines were developed. Based on the high expression in seeds, we performed GUS staining on the T_2 seeds of each transgenic line and screened three lines (*ProATL5:GUS*-5, -8, -14) with the strongest staining for subsequent expression analysis (Fig. S4).

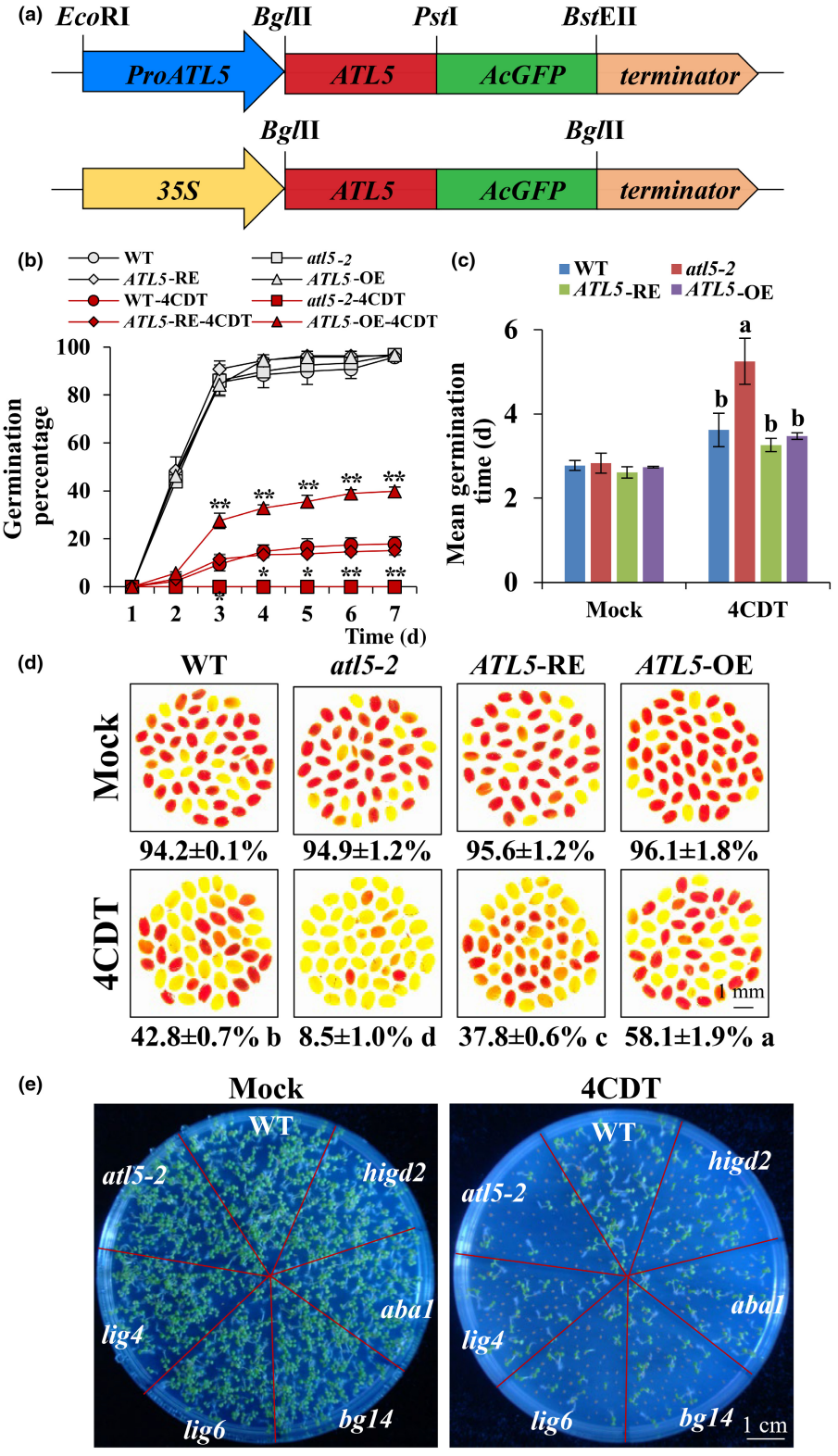

GUS staining of three *ProATL5:GUS* T_3 lines revealed a similar expression pattern in which *ATL5* was highly expressed in the leaves and roots of 10-d-old seedlings but significantly reduced as vegetative growth progressed, as seen in the leaves of 20-d-old plants, and showed no expression in the leaves of 30-d-old plants (Fig. 3b,I–III). *ATL5* was highly expressed in flowers and pods on the 5th and 10th days after flowering, and *ATL5* was expressed in both the embryo and endosperm of the seed until the mature

Fig. 2 ATL5 strongly and positively regulates seed longevity in *Arabidopsis*. (a) Schematic representation of the *ProATL5:ATL5-GFP* and *35S:ATL5-GFP* vectors. The *ATL5-GFP* fusion gene was driven by its self-promoter or 35S promoter, and the *Bar* gene was used as a selection marker. (b) Germination percentage and MGT (c) of wild-type (WT), *atl5-2* mutant, reversion (*ATL5*-RE) and overexpression (*ATL5*-OE) seeds at 7 days after moist chilling (DAM) without or with 4CDT. As two independent lines of *ATL5*-RE and *ATL5*-OE showed similar germination statuses, the mean values of each genotype group are shown here. Experiments were repeated three times, and values are shown as the mean ± SD. (d) Viable seed percentages without (Mock) or with 4CDT, analyzed using tetrazolium staining. Dark red indicates viable seeds. Bar, 1 mm. (e) Comparison of the ageing phenotype *of atl5-2* with other seed ageing mutants (*aba1*, *lig4*, *lig6*, *bg14*, and *higd2*, which were disrupted in zeaxanthin epoxidase, ligase IV, ligase VI, β-glucosidase 14 and hypoxia inducible gene domain family member 1, respectively). Germination status at 7 DAM without (mock) or with 4CDT. Bar, 1 cm. Data are shown as the mean ± SD ($n = 3$). Asterisks above or below the bars indicate significant differences with the respective control (*t*-test): *, $P < 0.05$; **, $P < 0.01$. Different lowercase letters above the bars or after the data indicate significant differences between genotypes at $P < 0.05$ based on ANOVA-S-N-K test.

stage (Fig. 3b,IV–XII). We also determined the ATL5 induction expression pattern. Upon aging induction, the expression of *ATL5*, which was present in both the embryo and endosperm, was significantly increased (Fig. 3c).

To further understand the function of ATL5, we studied its subcellular localization. The full-length open reading frame of ATL5 was cloned into the pHBT-GFP-NOS vector to produce pHBT-ATL5-GFP, and either pHBT-GFP and NLS-mCherry or pHBT-ATL5-GFP and NLS-mCherry (nuclear markers) were cotransformed into *Arabidopsis* protoplasts. The GFP signal was clearly detected in both the nucleus and the cytoplasm in the GFP control-transformed protoplast, while the GFP signal was detected only in the nucleus (colocalization with NLS marker) in the GFP-ATL5 transformed protoplast (Fig. 3d). Meanwhile, GFP was colocalized with mCHERRY in the nucleus regardless of whether it attached to ATL5 (Fig. 3d). These results suggested that ATL5 is located in the nucleus.

Identification of the proteins that interact with ATL5

To identify proteins targeted for ubiquitination by ATL5, a yeast two-hybrid screen against an *Arabidopsis* normalized cDNA library was performed. As the N-terminal transmembrane domain of ATL5 inhibited its adequate expression and nuclear localization in yeast (Sato *et al.*, 2011), the domain was removed and the remaining truncated ATL5 was fused to the yeast GAL4 BD domain as 'bait'. After sequential screening on SD-Trp-Leu-His and SD-Trp -Leu-His-Ade selective media, 90 positive clones were obtained. The β-galactosidase activity of each clone was assessed on SD-Trp-Leu-His-Ade medium containing X-α-Gal. The inserted sequences of the blue clones were amplified and sequenced. Twenty-four potential interacting proteins were identified (Table S2). According to the tissue-specific pattern and subcellular location, nine proteins, including ABT1 (Table S2), which contains a unique acidic domain and RNA recognition motif (RRM)_ABT1_like domain (Fig. S5), were chosen as candidates for reverse yeast two-hybrid analysis. ABT1 was so named due to its 79.5% homology with *Saccharomyces cerevisiae* ABT1 (Oda *et al.*, 2000; Fig. S5).

ATL5 physically interacts with ABT1 *in vitro* and *in vivo*

To confirm the interaction between ATL5 and ABT1, reverse yeast two-hybrid analysis was performed. ATL5 (without the N-terminal transmembrane domain) was fused to the yeast GAL4 AD domain, while full-length ABT1 was fused to the yeast GAL4 BD domain. Positive clones were formed in BD-ABT1/AD-ATL5 on SD-Trp-Leu-His-Ade medium, indicating that an interaction occurred between ATL5 and ABT1 in yeast cells (Fig. S6).

To more precisely identify the ATL5 region responsible for the interaction with ABT1, we fused two truncated ATL5 variants to the yeast GAL4 AD domain and three truncated ABT1 variants to the yeast GAL4 BD domain and analyzed the interactions between ATL5 or ABT1 and these derivatives. Deletion of the 105 C-terminal residues of ATL5 (AD-ATL$^{51–154}$) completely eliminated its interaction with ABTI, while deletion of the 104 N-terminal residues of ATL5 (AD-ATL5$^{153–257}$), including the RING domain, did not affect its interaction with ABT1 (Fig. 4a). These results indicate that the C-terminal residues of ATL5 are essential for its interaction with ABT1. Similarly, we analyzed the interaction of the truncated ABT1 with ATL5 and found that the deletion of both RRM and the C-terminal residues eliminated its interaction with ATL5, while inclusion of either RRM or the C-terminal residues was sufficient for interaction with ABT1, indicating that both RRM and the C-terminal residues are responsible for the interaction with ATL5 (Fig. 4b).

The physical interaction between ATL5 and ABT1 in plant cells was further corroborated with bimolecular fluorescence complementation (BiFC). ATL5 and ABT1 were fused to the C-terminus or N-terminus of the yellow fluorescent protein (YFP) fragment, resulting in pSPYC-ATL5 and pSPYN-ABT1. Coinfiltration of pSPYC-ATL5 and pSPYN-ABT1 in *Nicotiana benthamiana* leaf cells led to strong YFP fluorescence, whereas pSPYC-ATL5 or pSPYN-ABT1 coinfiltrated with empty vector showed no detectable YFP fluorescence (Fig. 4c). Importantly, ATL5 interacted with ABT1 in the nucleus, as the fluorescence signal merged with the signal from the protein product of the nuclear marker gene *NLS* (Fig. 4c). Moreover, the ATL5–ABT1 interaction was further confirmed by Co-IP assays in *N. benthamiana* leaves simultaneously expressing ATL5 and ABT1 (Fig. 4d). Taken together, our data demonstrate that ATL5 physically interacts with ABT1 in yeast and plant cells.

ATL5 mediates the polyubiquitination and degradation of ABT1 via the 26S proteasome pathway

To investigate whether ATL5 functions as an E3 ligase, we first determined its autoubiquitination activity *in vitro*. *ATL5* was

expressed in *E. coli* to produce a fusion protein with GST and was then affinity-purified from the soluble fraction of the bacterial lysate. Ubiquitination activity was analyzed using Western blotting. In the presence of E1, E2, GST-tagged ATL5 and ubiquitin, high-MW bands corresponding to the autoubiquitinated bands were present (Fig. 5a), while no autoubiquitinated bands were detected in the absence of either E1, E2, ATL5-GST or ubiquitin or in the presence of GST or bATL5-GST (boiled ATL5-GST; Fig. 5a). To further confirm the ubiquitination activity to ABT1, we expressed *ABT1-FLAG* and *ATL5-MYC* in *N. benthamiana* leaves. Then, proteins containing ABT1-FLAG and ATL5-MYC were extracted separately, and the ubiquitination activity was analyzed using Western blotting. In the presence of E1, E2, and ubiquitin in the reaction, high-MW bands corresponding to ubiquitinated ATL5 were present. When either component of E1, E2, or ATL5 was lacking, no ubiquitinated band was present (Fig. 5b). These results indicate that ATL5 displays ubiquitination activity *in vitro*.

To explore whether ATL5 could mediate the degradation of ABT1, *ATL5-MYC*, *ATL5C132A-MYC* (mutating Cys-132 to Ala in the RING domain), *ABT1-FLAG*, and *GFP-FLAG* were co-expressed in *N. benthamiana* leaves, and ABT1 abundance was determined by Western blotting. The levels of ABT1 protein were substantially decreased with increasing levels of ATL5-MYC, while ATL5-mediated degradation of ABT-FLAG was fully blocked when co-expressed with the control vector and ATL5C132A-MYC (Fig. 5c), demonstrating that the degradation of ABT1 is affected by the abundance of ATL5 and that the ring domain is essential for its function. To investigate whether ATL5-mediated degradation of ABT1 was dependent on the 26S proteasome, CHX and MG132, inhibitors of protein synthesis and the proteasome, respectively (Yu *et al.*, 2020), were used for the degradation assay. MG132 efficiently blocked the ATL5-mediated degradation of ABT1 (Fig. 5d).

Taken together, our data demonstrate that ATL5 functions as an E3 ligase and can mediate the ubiquitination of ABT1 *in vitro* and *in vivo*.

ABT1 is a target protein of ATL5 and exerts a negative role on seed longevity in *Arabidopsis*

The above results suggest that ATL5 targets and polyubiquitinates ABT1 for its degradation. If this is the case, genetically, ABT1 should act downstream of ATL5, and the *abt1* mutant should have the opposite seed longevity phenotype of *atl5-2*. To test this hypothesis, we isolated a T-DNA insertion mutant of *abt1* (SALK_044704C; Fig. S7a–c) and compared the germination percentage and MGT without and with CDT. The germination percentage of the *abt1* mutant was significantly higher than that of the WT, while *atl5-2* showed almost no germination after 4CDT (Fig. S7d,e). Meanwhile, MGTs in these genotypes were negatively correlated with their respective germination percentages after 4CDT (Fig. S7f). Moreover, we performed TTZ staining of the aged seeds. As expected, the percentage of *abt1* seeds that stained darker was significantly higher than that of WT seeds, while almost no *atl5-2* seeds were stained dark (Fig. S7g).

To further explore the genetic relationship of ATL5 and ABT1 in regulating seed longevity, we transformed *35S:ABT1-MYC* into WT and *atl5-2* and generated *ABT1*-OE and *ABT1*-OE/*atl5-2* transgenic plants, each selecting three lines (*ABT1*-OE/*atl5-2*-3, -6 and -7; *ABT1*-OE-2, -3 and -5) with the highest ABT1 expression for further studies (Fig. S8). Compared with WT plants, the germination percentage of *ABT1*-OE was significantly lower than that of the WT, which was in contrast to the phenotype of *abt1*. The expression *ABT1* in *atl5-2* (*ABT1*-OE/-*atl5-2* transgenic line) showed almost no germination after treatment (Fig. 6a,b). Meanwhile, MGTs in these genotypes (except *abt1*) were negatively correlated with their respective germination percentage after 4CDT (Fig. 6c). Moreover, the seed longevity phenotype in these genotypes corresponded well with the TTZ staining results (Fig. 6d).

Taken together, our data demonstrated that ABT1 is a target protein of ATL5 and exerts a negative effect on seed longevity in *Arabidopsis*.

ATL5 is required for seed ageing-induced degradation of ABT1

ATL5 mediating the *in vitro* polyubiquitination of ABT1 prompted us to investigate the *in vivo* regulation of ABT1 by ATL5. We first determined the ATL5 abundance in the ATL5-GFP OE seeds upon CDT. The ATL5 protein accumulated 1.92-fold in the 1CDT seeds, continuously increased as ageing progressed, and increased 3.28-fold in the 3CDT seeds, compared with the untreated seeds (Fig. 7a), indicating that ATL5 is a seed ageing induced protein. Then, we compared the endogenous ABT1 protein levels in the seeds of ABT1-MYC/WT and ABT1-MYC/*atl5-2* transgenic lines. Indeed, the ABT1 protein markedly accumulated to higher levels (almost double) in the ABT1-MYC/*atl5-2* seeds than in the ABT1-MYC/WT seeds (Fig. 7b), indicating that disruption of ATL5 in the *atl5-2* mutant diminished the turnover of ABT1-MYC.Moreover, we compared the protein dynamics of ABT1-MYC in the seeds of these transgenic lines with or without CDT. The ABT1-MYC level was lower in the mocked seeds than in the aged seeds, and the level in the aged seeds increased as the ageing progressed (Fig. 7c). The turnover of ABT1-MYC was markedly diminished in ABT1-MYC/*atl5-2* seeds compared with ABT1-MYC/WT aged seeds at each ageing time (Fig. 7c), indicating that turnover of ABT1 in response to CDT is dependent on ATL5 function.

To further investigate whether the degradation of ABT1 occurs via the 26S proteasome pathway, we treated the seeds without/with CDT, and then compared the protein dynamics of ABT1-MYC in the imbibed seeds without or with MG132 in the presence of CHX. Without CDT, we observed that MG132 blocked the degradation of the translated ABT1 protein in seeds of both genotypes (Fig. 7d), suggesting that other E3 ligases may be involved in the degradation of the ABT1 protein, while upon CDT, MG132 blocked the degradation of the translated ABT1 protein in WT seeds but not in *atl5-2* seeds (Fig. 7d), indicating that ATL5 mainly functions in seed aging-

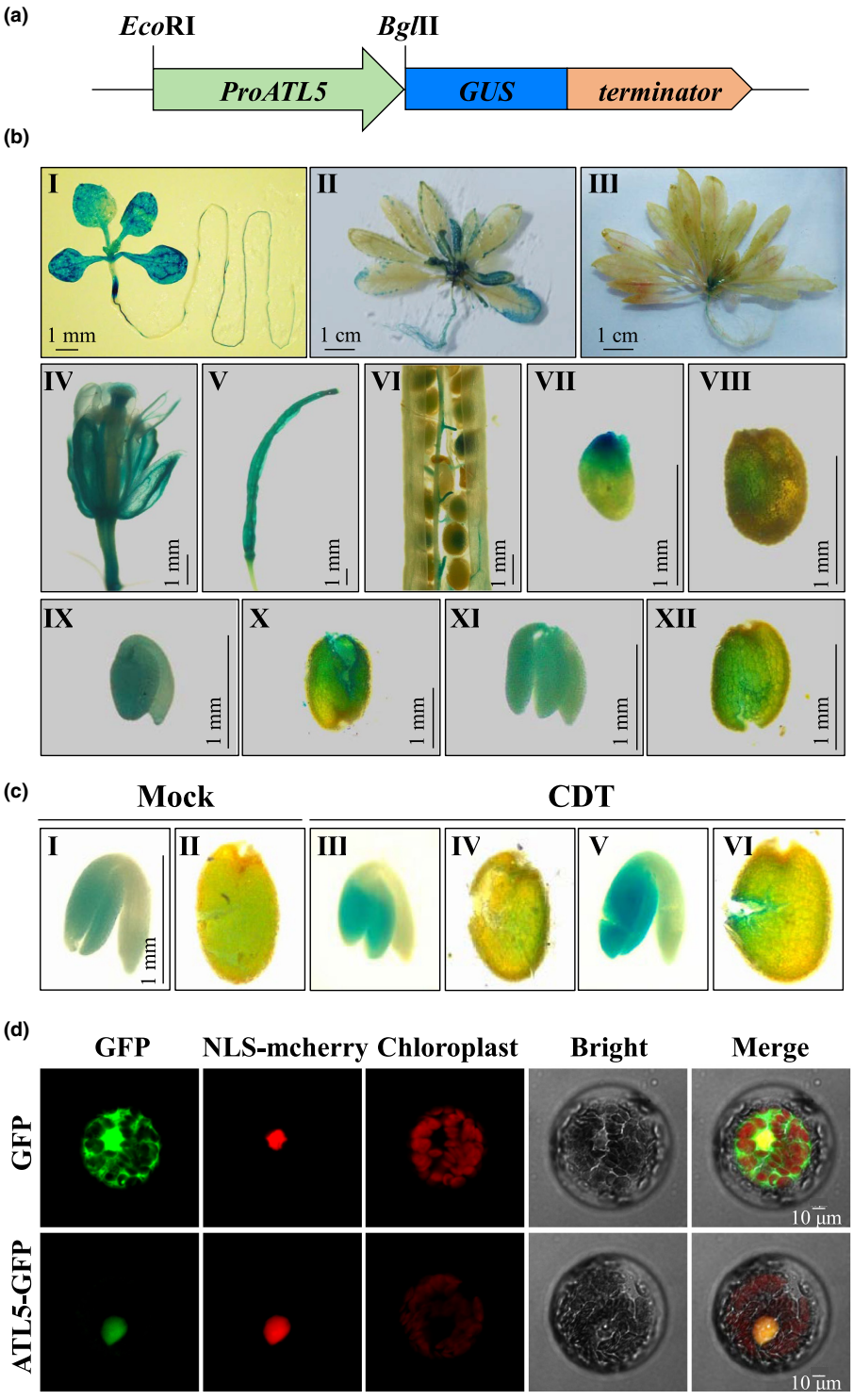

Fig. 3 Expression pattern of *ATL5*. (a) *ProATL5:GUS* vector diagram. (b) Tissue-specific expression of *ATL5* revealed by GUS staining. (I–III) Ten-, 20-, and 30-d-old seedlings; (IV) flowers, (V, VI) pods on the 5th and 10th days after flowering, (VII, VIII) seeds from 10- and 20-d-old pods; embryos (IX, XI) and seed coats with endosperm (X, XII) were separated from 10- and 20-d-old pods, respectively. (c) GUS staining analysis of embryos and seed coats of 20-d-old pods without (mock) or with CDT. (d) Subcellular localization of ATL5. *ATL5-GFP* and *GFP* (control) constructs were transformed into *Arabidopsis* protoplasts. NLS-mCherry was used as a nuclear marker. (d) Bars, 10 μm.

induced degradation of ABT1. Subsequently, we analyzed ABT1 at the transcriptional level and found that none of the above samples showed a difference in the transcriptional level of ABT1. Taken together, we conclude that ATL5 mediates ageing-induced ABT1 turnover via the 26S proteasome pathway in *Arabidopsis* seeds.

Discussion

Seed longevity is a crucial trait for both ecological and agronomic value. Polyu biquitination is a fundamental mechanism fine-regulating specific target protein degradation in eukaryotic cells. ATLs are a plant-specific ubiquitin ligase family that comprises

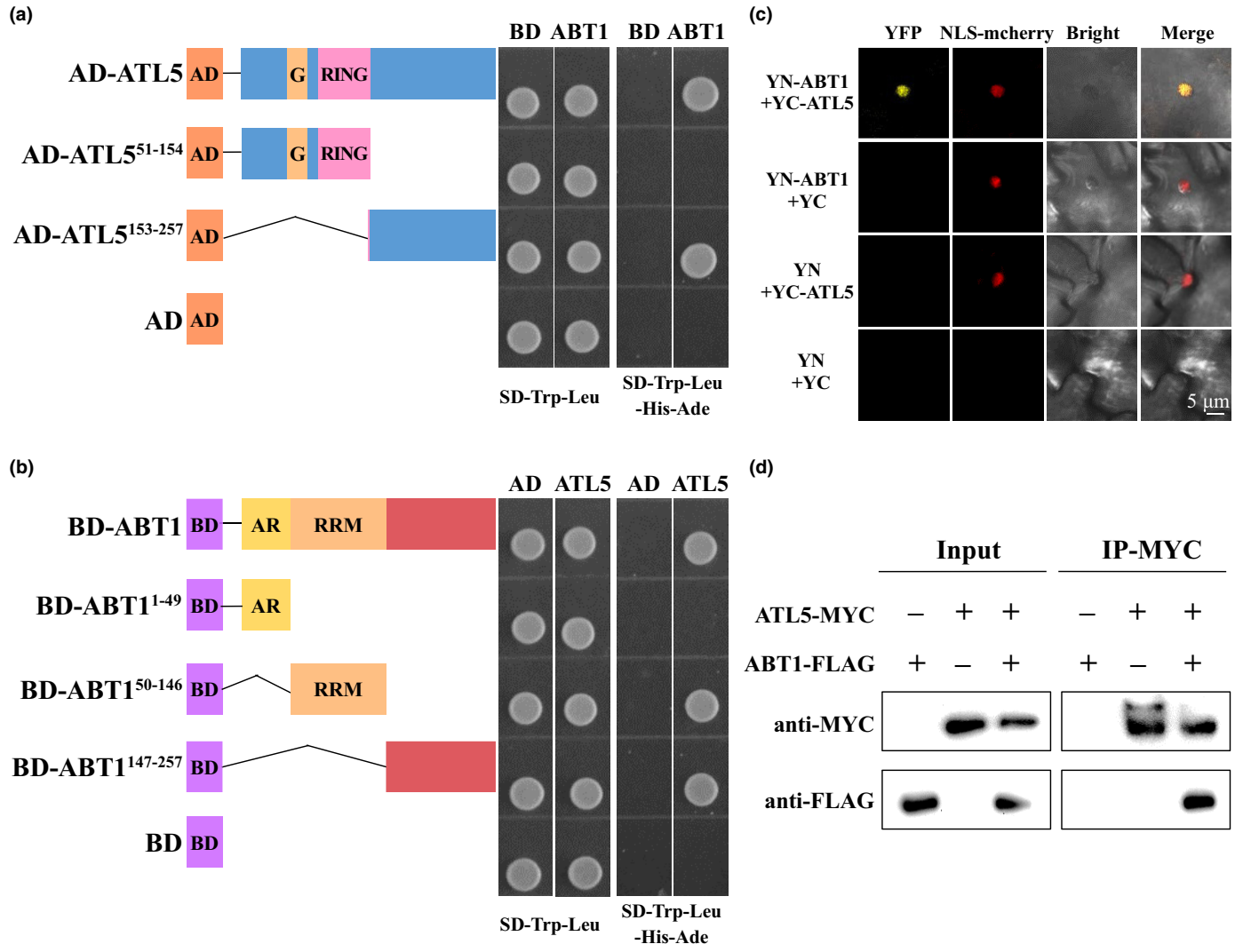

Fig. 4 ATL5 interacts with ABT1 *in vitro* and *in vivo*. (a) Identification of the domain of ATL5 that interacts with ABT1 revealed by a yeast two-hybrid assay. ATL5 without the N-terminal transmembrane domain or truncated domains was fused with GAL4-AD and cotransformed with BD-ABT1 into Y2H Gold yeast strains, and incubated on control medium (SD-Trp-Leu) or selective medium (SD-Trp-Leu-His-Ade). G, highly conserved motif containing Gly-Leu-Asp residues; RING, RING-H2 type zinc finger domain. pGADT7 (AD) and pGBKT7 (BD) vectors were used as negative controls. (b) Identification of the domain of ABT1 that interacts with ATL5 in a yeast two-hybrid assay. Full-length or truncated ABT1 was fused with GAL4-BD, and a yeast two-hybrid assay was performed as described in (a). AR, acidic region; RRM, RNA recognition motif (RRM) found in activator of basal transcription 1 (ABT1) and similar proteins. (c) Interaction of ATL5 with ABT1 in the BiFC assay. The indicated construct pairs were coexpressed in tobacco leaves for 3 d before images were taken. Bar, 5 μm. (d) Interaction of ATL5 with ABT1 revealed by Co-IP assay. Total protein was extracted from tobacco leaves expressing *35S: ATL5-MYC*, *35S: ABT1-FLAG*, or both for 3 d, and incubated with anti-MYC and protein A/G beads. ABT1-FLAG and ATL5-MYC were detected using anti-FLAG and anti-MYC antibodies, respectively.

91 members in the *Arabidopsis* genome (Smalle & Vierstra, 2004). Roles for several members of the family have been determined, including plant development (Pagnussat *et al.*, 2005), absorption and transport of mineral nutrients (Shin *et al.*, 2013; Suh & Kim, 2015), biotic (Serrano & Guzman, 2004; Deng *et al.*, 2017) and abiotic stress (Suh *et al.*, 2016) responses. Most of their functions, particularly in seed longevity, remain unknown. Here, we report ATL5, a previously uncharacterized *Arabidopsis* E3 ubiquitin ligase that contributes to the fine-tuning of seed longevity through polyubiquitination and proteasomal degradation of ABT1. This is also the first seed longevity-related ubiquitin ligase reported in *Arabidopsis*.

In this study, using the *atl5-2* mutant, we revealed that disruption of ATL5 resulted in a faster accelerated aging phenotype than WT (Fig. 1), while overexpressing *ATL5* in the *atl5-2* mutant (*ATL5*-RE) basically recovered the faster accelerated aging phenotype of *atl5-2* (Fig. 2b,c). Comparison of the phenotype of *atl5-2* with other seed-aging mutants (Waterworth *et al.*, 2010; Dekkers *et al.*, 2016) revealed that *atl5-2* presented the strongest phenotype among the detected mutants (Fig. 2d). Consistent with its function in seed longevity, the expression of *ATL5* gradually decreased as vegetative growth progressed but was highly expressed in the reproductive organs and embryos of mature seeds (Fig. 3b) and could be induced by accelerated aging

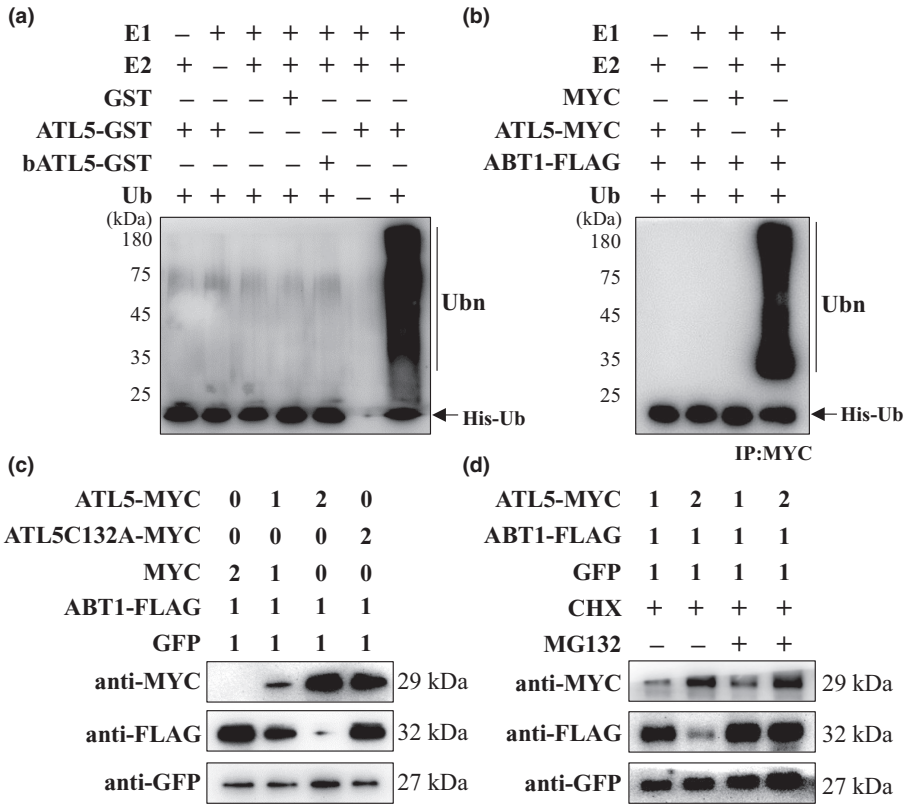

Fig. 5 ATL5 acts as an E3 ligase and promotes the ubiquitination and degradation of ABT1 via the 26S proteasome pathway. (a) *In vitro* analysis of the ubiquitination activity of ATL5. ATL5-GST and GST proteins were extracted from *Escherichia coli* cells and the ubiquitination reaction was determined in the absence of yeast Ub, yeast E1 (uba1), and yeast E2 (rad6) using an anti-Ub antibody. b-ATL5-GST: boiled ATL5-GST. (b) Semi-*in vitro* analysis of ATL5-mediated ubiquitination of ABT1. ABT1-FLAG and ATL5-MYC or MYC proteins were extracted from tobacco leaves and immunoprecipitated with MYC tag antibodies. The ubiquitination reaction was determined as described in (a). (c) ATL5 mediates the degradation of ABT1 *in planta*. Proteins were extracted from tobacco leaves 3 d after infiltration with different vectors. ATL5 and ATL5C132A proteins were detected with anti-MYC. ABT1 and GFP levels were detected with anti-FLAG and anti-GFP antibodies, respectively. GFP was used as an internal expression control. (d) ATL5-mediated ABT1 degradation was inhibited by MG132. Proteins were extracted from tobacco leaves after treatment with 50 μM CHX and MG132 before sampling. Western blotting was performed as described in (c).

(Fig. 3c). These data clearly demonstrated that *ATL5* strongly and positively regulates seed longevity in *Arabidopsis*.

To further reveal the mechanism by which ATL5 regulates seed longevity, we obtained a polyubiquitinated target of ABT1 against a normalized *Arabidopsis* cDNA yeast two hybrid library with ATL5 as a bait (Table S2). The interaction of ATL5 and ABT1 was further confirmed in reverse yeast two-hybrid analysis (Fig. S6) and Co-IP assays (Fig. 4d), and the proteins colocalized specifically in the plant cell nucleus in the *in vivo* BiFC system (Fig. 4c). Interestingly, the interaction occurred in the C-terminal region of ATL5 and the C-terminal region of ABT1 (Fig. 4a), but not in the active centers in ATL5 (RING domain) and ABT1 (acidic activator region; Jiang & Eberhardt, 1996), which is consistent with the finding that ATL31 interacts with 14-3-3χ on the C-terminal region in response to C/N-nutrient conditions (Sato *et al.*, 2011). It was reported that ATL31 phosphorylation on the Ser/Thr residues of the C-terminal region of ATL31 has dual effects on ATL31 stabilization and 14-3-3χ binding (Liu *et al.*, 2022). Therefore, additional studies are required to clarify the regulatory mechanism, including phosphorylation, underlying the targeting of the ubiquitin ligase ATL5 to the ABT1 protein.

Moreover, *in vitro* and semi-*in vivo* ubiquitination assays in the presence of ubiquitin, yeast E1 (uba1), and yeast E2 (rad6) revealed that GST-tagged ATL5 was clearly autoubiquitinated and displayed E3 ligase activity (Fig. 5a,b). Consistent with this, semi *in vivo* analysis revealed that the accumulation of ABT1 was significantly diminished in the presence of ATL5, which was also inhibited by proteasomal inhibitor MG132 (Fig. 5c,d). The degradation of ABT1 was completely abolished if the conserved Cys-132 to Ala in the RING domain of ATL5 was mutated (Fig. 5c), which is also seen in a number of other RING domain E3 ligase activities in ATL family members (Sato *et al.*, 2011). However, although the ubiquitination of the ATL5 protein was verified in the presence of yeast rad6 as an E2 protein, the real interactive E2 protein for ATL5 proteins in *Arabidopsis* remains unknown.

The function of ABT1 was only identified in yeast, and ABT1 is essential for the generation of viable spores (Oda *et al.*, 2000). It was reported that yeast ABT1 is a novel TBP binding protein

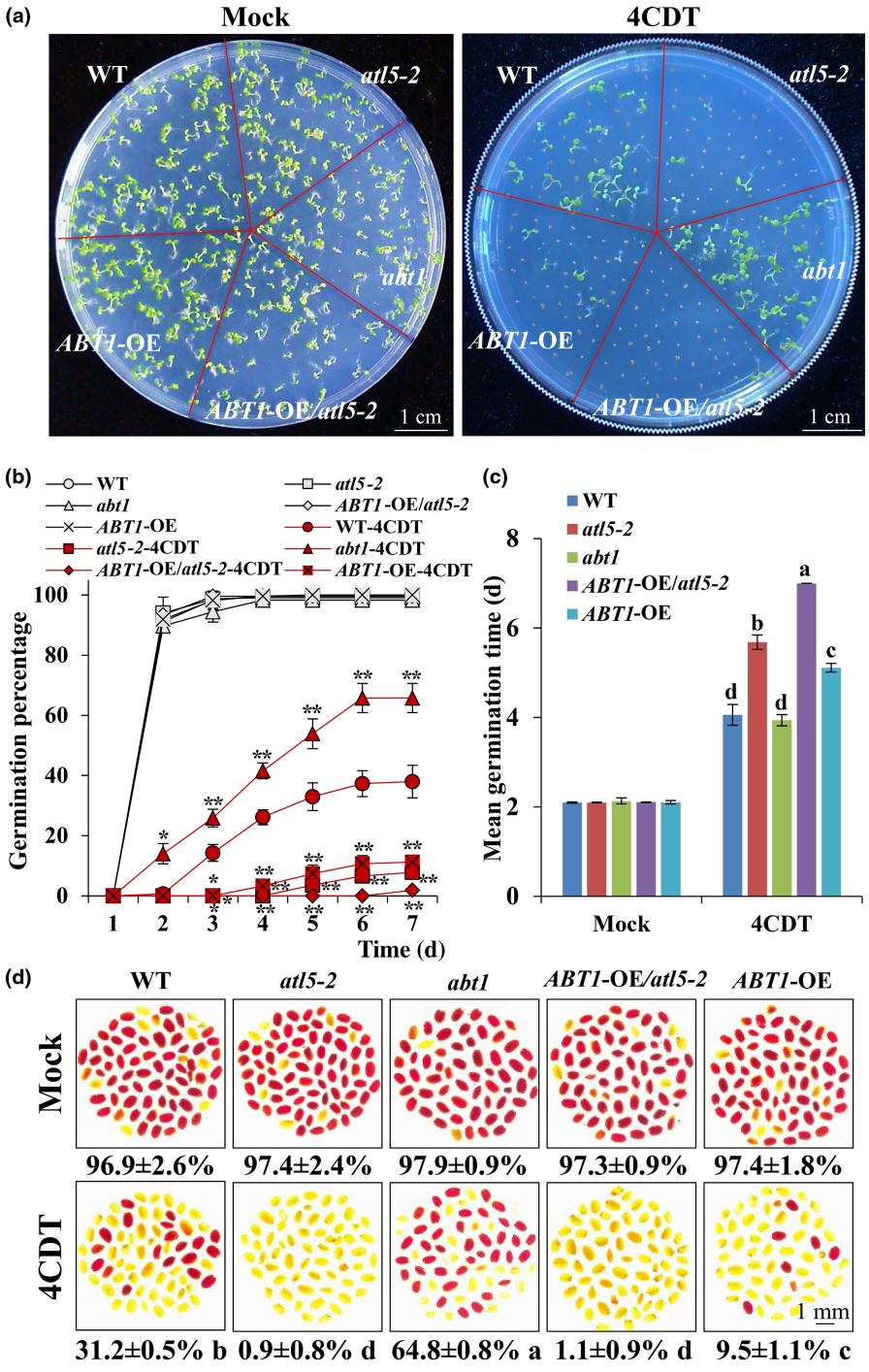

Fig. 6 Loss of function of ABT1 recovers the impaired seed longevity in *Arabidopsis*. (a) Germination status, (b) percentage and (c) MGT of wild-type (WT), *atl5-2*, *abt1*, *ABT1*-OE/*atl5-2* and *ABT1*-OE seeds at 7 DAM without (mock) or with CDT. As three independent lines of *ABT1*-OE/*atl5-2* and *ABT1*-OE showed similar germination statuses, the mean values of each genotype group are shown here for simplicity. Experiments were repeated three times, and values are shown as the mean ± SD. Bar, 1 cm. (d) Viable seed percentages of WT, *atl5-2*, *abt1*, *ABT1*-OE/*atl5-2* and *ABT1*-OE without (Mock) or with CDT analyzed using tetrazolium staining. Dark red indicates viable seeds. Bar, 1 mm. Data are shown as the mean ± SD ($n = 3$). Asterisks above or below the bars indicate significant differences with the respective control (*t*-test): *, $P < 0.05$; **, $P < 0.01$. Different lowercase letters above the bars or after the data indicate significant differences between genotypes at $P < 0.05$ based on ANOVA-S-N-K test.

and could promote Pol II-mediated basal transcription *in vitro* and in HeLa cells (Oda *et al.*, 2000). In this study, we demonstrated that *Arabidopsis* ATB1 is a negative regulator of seed longevity, since overexpression of ABT1 significantly decreased seed longevity (Fig. 6), while disruption of ABT1 in the *abt1* mutant increased seed longevity (Figs 6, S7). Furthermore, the amount of translated ABT1 proteins increased as seeds were subjected to ageing treatment in WT *Arabidopsis* seeds (Fig. 7b), and this was enhanced in the *atl5-2* mutant background (Fig. 7b). Moreover, the amount of ABT1 present in seeds, regardless of ageing, increased in the presence of the potent proteasomal inhibitor MG132 and the translational inhibitor CHX (Fig. 7c). Therefore, our data provide a direct link between the ATL5-mediated proteasomal degradation of ATB1 and seed longevity in *Arabidopsis*. However, we could not find an interaction of *Arabidopsis* ATB1 with either TBP1 or TBP2 in yeast two-hybrid analysis (Fig. S9), which is in contrast to the observation in yeast ABT1 (Oda *et al.*, 2000).

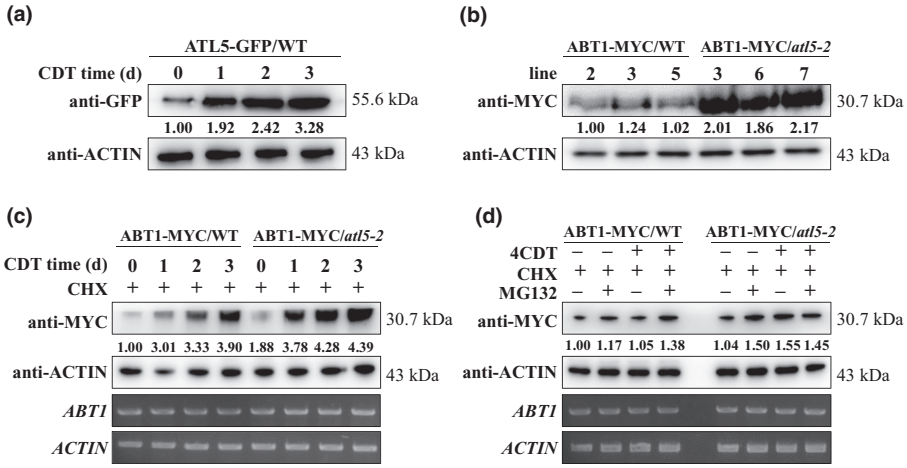

Fig. 7 ATL5 is required for seed aging-induced degradation of ABT1. (a) The ABT-MYC protein level was increased after controlled deterioration treatment (CDT). (b) ABT1-MYC protein levels in seeds of ABT1-MYC/WT and ABT1-MYC/*atl5-2* transgenic lines after harvesting for 1 month. (c) Kinetics of ABT1-MYC degradation upon ageing treatment. (d) ATL5-mediated ABT1 degradation was inhibited by MG132. In (c, d), seeds without or with CDT were placed in liquid 1/2 MS medium containing 50 μM CHX and/or 50 μM MG132 and cultured at 22°C for 2 h. An equal volume of DMSO was used as a control. ABT1-MYC and Actin protein levels in seeds were detected by western blotting using anti-MYC and anti-Actin antibodies, respectively. Actin was used as an internal expression control. The expression of targeted genes and *ACTIN1* was analyzed by RT–PCR (bottom panels).

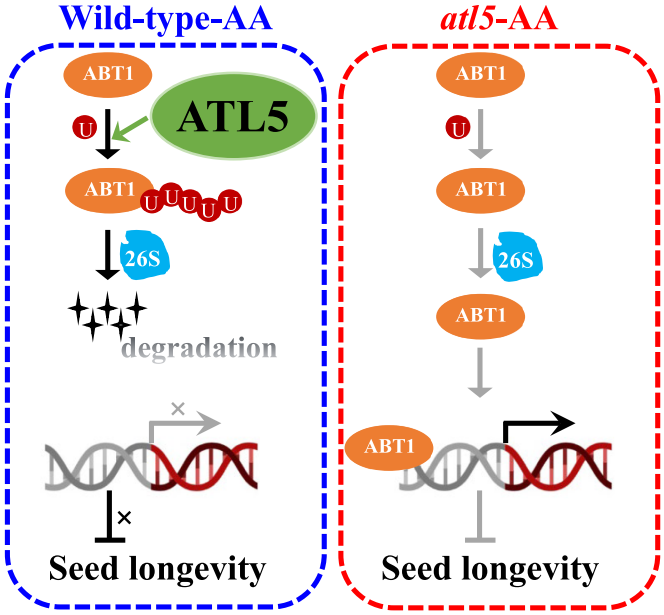

Fig. 8 Proposed model for ATL5-mediated regulation of seed longevity in *Arabidopsis*. ABT1 protein accumulates in seeds as ageing progresses. During this process, ATL5 is induced and promotes the ubiquitination and degradation of ABT1, which does not activate the transcription of the original downstream genes, and minimizes the negative effects on seed longevity, thereby enhancing seed longevity. When ATL5 is disrupted, the ubiquitination and degradation of ABT1 are blocked. ABT1 activates the transcription of downstream genes that are negatively involved in seed longevity, and thereby reduces seed longevity. Black arrow: positive regulation. Blunt end: negative regulation. Grey arrow and Cross: not happened.

Regulation of transcription via ubiquitination of transcription factors has been substantially reported in animal and plant cells. The ubiquitination of transcription factors could modify their stability, subcellular localization, and activity, such as plant U-Box40 degrading BRASSINAZOLE RESISTANT1 (BZR1; Kim *et al.*, 2019), and MORE AXILLARY GROWTH2 (MAX2) targeting SMAX1-LIKE (SMXL; Wang *et al.*, 2020). However, there are no reports about the ubiquitin-mediated degradation of basal transcription activators that carry an acidic activation domain in plants. Such transcription activators usually interact with an impressive array of basal transcription factor apparatuses (Hope & Struhl, 1986). When they are expressed at high levels, they mitigate transcriptional activation by sequestering basal transcription factors away from productive promoter complexes (Gill & Ptashne, 1988). Moreover, a close relationship was observed between the ability of such transcription activators to activate transcription and the efficiency with which they are destroyed by polyubiquitin-mediated proteolysis (Salghetti *et al.*, 2000). Thus, the polyubiquitin-mediated proteolysis of basal transcription activator is a precise mechanism to block the activity of such an activator and minimize its negative role in eukaryotes. Therefore, our findings provide new insights into the regulation of the basal transcription activator ABT1 in seed longevity. However, as a number of mechanisms are involved in seed longevity, and ABT1 may affect seed longevity through a novel mechanism that has not been reported, it is difficult to know the exact mechanism by which ABT1 affects seed longevity in *Arabidopsis*. How ABT1 negatively affects seed longevity and which downstream genes are regulated transcriptionally needs further research.

In conclusion, an uncharacterized ATL family member, ATL5, was identified to interact with ABT1. When seeds are aged, ATL5 promotes the polyubiquitination and degradation of ABT1, which prevents the transcription of original downstream genes, minimizing negative effects and thereby enhancing seed longevity. When ATL5 is disrupted, the polyubiquitination and degradation of ABT1 is blocked. ABT1 activates the transcription of downstream genes that are negatively involved in seed longevity and thereby reduces seed longevity (Fig. 8). Our finding that ATL5 regulates

seed longevity-related ABT1 transcriptional activation provides the first description of a RING E3 ubiquitin ligase that directly controls the basal transcriptional activation associated with seed longevity.

Acknowledgements

This work was supported by grants from the National Natural Science Foundation of China (nos. 32070349 and 31870304), the Natural Science Foundation of Tianjin (no. 21JCYBJC00010).

Competing interests

None declared.

Author contributions

DC and XC planned and designed the research. WH, RW, QZ, MF and SC performed the experiments. WH, MF, DC and XC analyzed the data. MF and YL drew the figs. DC and XC wrote the manuscript. All authors reviewed, revised, and approved the manuscript.

ORCID

Defu Chen https://orcid.org/0000-0002-1742-6011
Xiwen Chen https://orcid.org/0000-0002-6511-4709

Data availability

Data are available in article Supporting Information.

References

Chen DF, Li YN, Fang T, Shi XL, Chen XW. 2016. Specific roles of tocopherols and tocotrienols in seed longevity and germination tolerance to abiotic stress in transgenic rice. *Plant Science* **244**: 31–39.

Christian JO, Braginets R, Schulze WX, Walther D. 2012. Characterization and prediction of protein phosphorylation hotspots in *Arabidopsis thaliana*. *Frontiers in Plant Science* **3**: 207.

Ciechanover A. 2015. The unraveling of the ubiquitin system. *Nature Reviews Molecular Cell Biology* **16**: 322–324.

Clerkx EJ, Vries HB, Ruys GJ, Groot SP, Koornneef M. 2003. Characterization of green seed, an enhancer of *abi3-1* in *Arabidopsis* that affects seed longevity. *Plant Physiology* **132**: 1077–1084.

Clough SJ, Bent AF. 1998. Floral dip: a simplified method for *Agrobacterium*-mediated transformation of *Arabidopsis thaliana*. *The Plant Journal* **16**: 735–743.

Dekkers BJ, He H, Hanson J, Willems LA, Jamar DC, Cueff G, Rajjou L, Hilhorst HW, Bentsink L. 2016. The *Arabidopsis* DELAY of GERMINATION 1 gene affects ABSCISIC ACID INSENSITIVE 5 (ABI5) expression and genetically interacts with ABI3 during *Arabidopsis* seed development. *The Plant Journal* **85**: 451–465.

Deng F, Guo T, Lefebvre M, Scaglione S, Antico CJ, Jing T, Yang X, Shan W, Ramonell KM. 2017. Expression and regulation of ATL9, an E3 ubiquitin ligase involved in plant defense. *PLoS ONE* **12**: e188458.

Downie B, Gurusinghe S, Dahal P, Thacker RR, Snyder JC, Nonogaki H, Yim K, Fukanaga K, Alvarado V, Bradford KJ. 2003. Expression of a GALACTINOL SYNTHASE gene in tomato seeds is up-regulated before maturation desiccation and again after imbibition whenever radicle protrusion is prevented. *Plant Physiology* **131**: 1347–1359.

Gao M, He Y, Yin X, Zhong X, Yan B, Wu Y, Chen J, Li X, Zhai K, Huang Y *et al.* 2021. Ca^{2+} sensor-mediated ROS scavenging suppresses rice immunity and is exploited by a fungal effector. *Cell* **184**: 5391–5404.

Gill G, Ptashne M. 1988. Negative effect of the transcriptional activator GAL4. *Nature* **334**: 721–724.

Heiss G, Ploetz E, Voith VVL, Viswanathan R, Glaser S, Schluesche P, Madhira S, Meisterernst M, Auble DT, Lamb DC. 2019. Conformational changes and catalytic inefficiency associated with Mot1-mediated TBP-DNA dissociation. *Nucleic Acids Research* **47**: 2793–2806.

Hershko A, Ciechanover A. 1998. The ubiquitin system. *Annual Review of Biochemistry* **67**: 425–479.

Hope IA, Struhl K. 1986. Functional dissection of a eukaryotic transcriptional activator protein, GCN4 of yeast. *Cell* **46**: 885–894.

Jeevan KS, Rajendra PS, Banerjee R, Thammineni C. 2015. Seed birth to death: dual functions of reactive oxygen species in seed physiology. *Annals Botany* **116**: 663–668.

Jiang SW, Eberhardt NL. 1996. TEF-1 transrepression in BeWo cells is mediated through interactions with the TATA-binding protein, TBP. *Journal of Biological Chemistry* **271**: 9510–9518.

Kim EJ, Lee SH, Park CH, Kim SH, Hsu CC, Xu S, Wang ZY, Kim SK, Kim TW. 2019. Plant U-Box40 mediates degradation of the brassinosteroid-responsive transcription factor BZR1 in *Arabidopsis* roots. *Plant Cell* **31**: 791–808.

Kotak S, Vierling E, Baumlein H, von Koskull-Doring P. 2007. A novel transcriptional cascade regulating expression of heat stress proteins during seed development of *Arabidopsis*. *Plant Cell* **19**: 182–195.

Leprince O, Pellizzaro A, Berriri S, Buitink J. 2017. Late seed maturation: drying without dying. *Journal of Experimental Botany* **68**: 827–841.

Li F, Asami T, Wu X, Tsang EW, Cutler AJ. 2007. A putative hydroxysteroid dehydrogenase involved in regulating plant growth and development. *Plant Physiology* **145**: 87–97.

Li Y, Sun D, Ma Z, Yamaguchi K, Wang L, Zhong S, Yan X, Shang B, Nagashima Y, Koiwa H *et al.* 2020. Degradation of SERRATE via ubiquitin-independent 20S proteasome to survey RNA metabolism. *Nature Plants* **6**: 970–982.

Liu H, Ravichandran S, Teh OK, McVey S, Lilley C, Teresinski HJ, Gonzalez-Ferrer C, Mullen RT, Hofius D, Prithiviraj B *et al.* 2017. The RING-type E3 ligase XBAT35.2 is involved in cell death induction and pathogen response. *Plant Physiology* **175**: 1469–1483.

Liu L, Zhang Y, Tang S, Zhao Q, Zhang Z, Zhang H, Dong L, Guo H, Xie Q. 2010. An efficient system to detect protein ubiquitination by agroinfiltration in *Nicotiana benthamiana*. *The Plant Journal* **61**: 893–903.

Liu X, Zhou Y, Du M, Liang X, Fan F, Huang G, Zou Y, Bai J, Lu D. 2022. The calcium-dependent protein kinase CPK28 is targeted by the ubiquitin ligases ATL31 and ATL6 for proteasome-mediated degradation to fine-tune immune signaling in *Arabidopsis*. *Plant Cell* **34**: 679–697.

Maeda R, Tamashiro H, Takano K, Takahashi H, Suzuki H, Saito S, Kojima W, Adachi N, Ura K, Endo T *et al.* 2017. TBP-like protein (TLP) disrupts the p53-MDM2 interaction and induces long-lasting p53 activation. *Journal of Biological Chemistry* **292**: 3201–3212.

Matthews S, Khajeh-Hosseini M. 2007. Length of the lag period of germination and metabolic repair explain vigour differences in seed lots of maize (*Zea mays*). *Seed Science and Technology* **35**: 200–212.

Morris K, Thornber S, Codrai L, Richardson C, Craig A, Sadanandom A, Thomas B, Jackson S. 2010. DAY NEUTRAL FLOWERING represses CONSTANS to prevent *Arabidopsis* flowering early in short days. *Plant Cell* **22**: 1118–1128.

Murray M, Thompson W. 1980. Rapid isolation of high molecular weight plant DNA. *Nucleic Acids Research* **8**: 4321–4325.

Murthy UM, Sun WQ. 2000. Protein modification by Amadori and Maillard reactions during seed storage: roles of sugar hydrolysis and lipid peroxidation. *Journal of Experimental Botany* **51**: 1221–1228.

Nakajima S, Ito H, Tanaka R, Tanaka A. 2012. Chlorophyll b reductase plays an essential role in maturation and storability of *Arabidopsis* seeds. *Plant Physiology* **160**: 261–273.

Oda T, Fukuda A, Hagiwara H, Masuho Y, Muramatsu M, Hisatake K, Yamashita T. 2004. ABT1-associated protelin (ABTAP), a novel nuclear

protein conserved from yeast to mammals, represses transcriptional activation by ABT1. *Journal of Cellular Biochemistry* **93**: 788–806.

Oda T, Kayukawa K, Hagiwara H, Yudate HT, Masuho Y, Murakami Y, Tamura T, Muramatsu M. 2000. A novel TATA-binding protein-binding protein, ABT1, activates basal transcription and has a yeast homolog that is essential for growth. *Molecular and Cellular Biology* **20**: 1407–1418.

Pagnussat GC, Yu HJ, Ngo QA, Rajani S, Mayalagu S, Johnson CS, Capron A, Xie LF, Ye D, Sundaresan V. 2005. Genetic and molecular identification of genes required for female gametophyte development and function in *Arabidopsis*. *Development* **132**: 603–614.

Rajjou L, Belghazi M, Catusse J, Oge L, Arc E, Godin B, Chibani K, Ali-Rachidi S, Collet B, Grappin P *et al.* 2011. Proteomics and posttranslational proteomics of seed dormancy and germination. *Methods in Molecular Biology* **773**: 215–236.

Rao V, Petla BP, Verma P, Salvi P, Kamble NU, Ghosh S, Kaur H, Saxena SC, Majee M. 2018. Arabidopsis SKP1-like protein13 (ASK13) positively regulates seed germination and seedling growth under abiotic stress. *Journal of Experimental Botany* **69**: 3899–3915.

Reeves WM, Lynch TJ, Mobin R, Finkelstein RR. 2011. Direct targets of the transcription factors ABA-Insensitive(ABI)4 and ABI5 reveal synergistic action by ABI4 and several bZIP ABA response factors. *Plant Molecular Biology* **75**: 347–363.

Renard J, Ninoles R, Martinez-Almonacid I, Gayubas B, Mateos-Fernandez R, Bissoli G, Bueso E, Serrano R, Gadea J. 2020. Identification of novel seed longevity genes related to oxidative stress and seed coat by genome-wide association studies and reverse genetics. *Plant, Cell & Environment* **43**: 2523–2539.

Salghetti SE, Muratani M, Wijnen H, Futcher B, Tansey WP. 2000. Functional overlap of sequences that activate transcription and signal ubiquitin-mediated proteolysis. *Proceedings of the National Academy of Sciences, USA* **97**: 3118–3123.

Sano N, Rajjou L, North HM, Debeaujon I, Marion-Poll A, Seo M. 2016. Staying alive: molecular aspects of seed longevity. *Plant and Cell Physiology* **57**: 660–674.

Sato T, Maekawa S, Yasuda S, Sonoda Y, Katoh E, Ichikawa T, Nakazawa M, Seki M, Shinozaki K, Matsui M *et al.* 2009. CNI1/ATL31, a RING-type ubiquitin ligase that functions in the carbon/nitrogenresponse for growth phase transition in *Arabidopsis* seedlings. *The Plant Journal* **60**: 852–864.

Sato T, Maekawa S, Yasuda S, Domeki Y, Sueyoshi K, Fujiwara M, Fukao Y, Goto DB, Yamaguchi J. 2011. Identification of 14-3-3 proteins as a target of ATL31 ubiquitin ligase, a regulator of the C/N response in *Arabidopsis*. *The Plant Journal* **68**: 137–146.

Serrano M, Guzman P. 2004. Isolation and gene expression analysis of *Arabidopsis thaliana* mutants with constitutive expression of ATL2, an early elicitor-response RING-H2 zinc-finger gene. *Genetics* **167**: 919–929.

Shin LJ, Lo JC, Chen GH, Callis J, Fu H, Yeh KC. 2013. IRT1 degradation factor1, a ring E3 ubiquitin ligase, regulates the degradation of iron-regulated transporter1 in *Arabidopsis*. *Plant Cell* **25**: 3039–3051.

Smalle J, Vierstra RD. 2004. The ubiquitin 26S proteasome proteolytic pathway. *Annual Review of Plant Biology* **55**: 555–590.

de Souza VD, Willems L, van Arkel J, Dekkers B, Hilhorst H, Bentsink L. 2016. Galactinol as marker for seed longevity. *Plant Science* **246**: 112–118.

Suh JY, Kim SJ, Oh TR, Cho SK, Yang SW, Kim WT. 2016. *Arabidopsis* Toxicos en Levadura 78 (AtATL78) mediates ABA-dependent ROS signaling in response to drought stress. *Biochemical and Biophysical Research Communications* **469**: 8–14.

Suh JY, Kim WT. 2015. *Arabidopsis* RING E3 ubiquitin ligase AtATL80 is negatively involved in phosphate mobilization and cold stress response in sufficient phosphate growth conditions. *Biochemical and Biophysical Research Communications* **463**: 793–799.

Verdier J, Lalanne D, Pelletier S, Torres-Jerez I, Righetti K, Bandyopadhyay K, Leprince O, Chatelain E, Vu BL, Gouzy J *et al.* 2013. A regulatory network-based approach dissects late maturation processes related to the acquisition of desiccation tolerance and longevity of *Medicago truncatula* seeds. *Plant Physiology* **163**: 757–774.

Waadt R, Kudla J. 2008. *In planta* visualization of protein interactions using bimolecular fluorescence complementation (BiFC). *Cold Spring Harbor Protocols* **2008**: t4995.

Wang L, Patrick JW, Ruan YL. 2018. Live long and prosper: roles of sugar and sugar polymers in seed vigor. *Molecular Plant* **11**: 1–3.

Wang L, Xu Q, Yu H, Ma H, Li X, Yang J, Chu J, Xie Q, Wang Y, Smith SM *et al.* 2020. Strigolactone and karrikin signaling pathways elicit ubiquitination and proteolysis of SMXL2 to regulate hypocotyl elongation in *Arabidopsis*. *Plant Cell* **32**: 2251–2270.

Wang WQ, Xu DY, Sui YP, Ding XH, Song XJ. 2022. A multiomic study uncovers a bZIP23-PER1A-mediated detoxification pathway to enhance seed vigor in rice. *Proceedings of the National Academy of Sciences, USA* **119**: e2026355119.

Waterworth WM, Masnavi G, Bhardwaj RM, Jiang Q, Bray CM, West CE. 2010. A plant DNA ligase is an important determinant of seed longevity. *The Plant Journal* **63**: 848–860.

Wiebach J, Nagel M, Borner A, Altmann T, Riewe D. 2020. Age-dependent loss of seed viability is associated with increased lipid oxidation and hydrolysis. *Plant, Cell & Environment* **43**: 303–314.

Yoo SD, Cho YH, Sheen J. 2007. *Arabidopsis* mesophyll protoplasts: a versatile cell system for transient gene expression analysis. *Nature Protocols* **2**: 1565–1572.

Yu F, Cao X, Liu G, Wang Q, Xia R, Zhang X, Xie Q. 2020. ESCRT-I component VPS23A is targeted by E3 ubiquitin ligase XBAT35 for proteasome-mediated degradation in modulating ABA signaling. *Molecular Plant* **13**: 1556–1569.

Supporting Information

Additional Supporting Information may be found online in the Supporting Information section at the end of the article.

Dataset S1 MS Excel table with individual sheets providing data that support the finding of this study.

Fig. S1 Screening of transgenic *ATL5*-RE and *ATL5*-OE lines.

Fig. S2 ATL5 strongly and positively regulates seed longevity in *Arabidopsis*.

Fig. S3 Growth and development of WT, *atl5-2* mutant, *ATL5*-RE, and *ATL5*-OE.

Fig. S4 Screening of *proATL5:GUS* transgenic plants.

Fig. S5 Sequence alignment of *Arabidopsis* ABT1 protein with other homologous proteins.

Fig. S6 Interaction of ATL5 with ABT1 in a yeast two-hybrid assay.

Fig. S7 *abt1* mutant showed enhanced seed longevity in *Arabidopsis*.

Fig. S8 Analysis of transgenic *ABT1* lines in *atl5-2* (*ABT1*-OE/*atl5-2*) and *ABT1* overexpression (*ABT1*-OE/WT) lines.

Fig. S9 Interaction of ABT1 with TBP1 or TBP2 in a yeast two-hybrid assay.

Table S1 Primers used in this study.

Table S2 Putative interacting proteins of ATL5 identified by yeast two-hybrid assay.

Please note: Wiley is not responsible for the content or functionality of any Supporting Information supplied by the authors. Any queries (other than missing material) should be directed to the *New Phytologist* Central Office.